Coupling of Pressure-Induced Structural Shifts to Spectral Changes in a Yellow Fluorescent Protein

Buz Barstow,[‡] Nozomi Ando,[§] Chae Un Kim,[†] and Sol M. Gruner[†§*]
[†]Cornell High Energy Synchrotron Source, [‡]School of Applied Physics, and [§]Department of Physics, Cornell University, Ithaca, New York

ABSTRACT X-ray diffraction analysis of pressure-induced structural changes in the *Aequorea* yellow fluorescent protein Citrine reveals the structural basis for the continuous fluorescence peak shift from yellow to green that is observed on pressurization. This fluorescence peak shift is caused by a reorientation of the two elements of the Citrine chromophore. This study describes the structural linkages in Citrine that are responsible for the local reorientation of the chromophore. The deformation of the Citrine chromophore is actuated by the differential motion of two clusters of atoms that compose the β-barrel scaffold of the molecule, resulting in a slight bending of the β-barrel. The high-pressure structures also show a perturbation of the hydrogen bonding network that stabilizes the excited state of the Citrine chromophore. The perturbation of this network is implicated in the reduction of fluorescence intensity of Citrine. The blue-shift of the Citrine fluorescence spectrum resulting from the bending of the β-barrel provides structural insight into the transient blue-shifting of isolated yellow fluorescent protein molecules under ambient conditions and suggests mechanisms to alter the time-dependent behavior of Citrine under ambient conditions.

INTRODUCTION

It has long been appreciated that the three-dimensional structure of a protein molecule can exert a strong influence over the active site of the molecule (1). This linkage permits allosteric binding of ligands and processing of substrates. Examples of this include the R to T transition in hemoglobin (1), the allosteric inhibition of phosphofructokinase by phosphoenolpyruvate (2), and the gating of ion channels (3). Small structural changes, sometimes <1 Å in magnitude, in a distant part of the molecule may be communicated through the protein matrix to an active and/or binding site, promoting a change in binding constant, catalytic rate, or other functional change.

Although allosteric effects in protein molecules are the most common example of the coupling between the overall structure of a protein molecule and its active sites, they are not the only example of effects of this type. Protein atomic structures solved at pressures up to a few hundred MPa (4–13) indicate that atoms in protein molecules are typically displaced by $\approx$0.1–1 Å from their ambient pressure positions. Pressures in the same range also significantly modify protein function (14). For example, the flash decay rate of firefly luciferase is reduced (15), the R to T transition in human hemoglobin is biased (16) and oxidation rates by morphinone reductase are substantially increased (17). The results from these studies suggest that subtle changes in protein structure caused by pressure can have a profound effect on function. However, specific details on the exact linkages that are involved in the coupling of structure and function as a function of pressure have been lacking.

To systematically investigate the effect of pressure on protein structure and function, we studied the *Aequorea* yellow fluorescent protein (YFP) (18,19) variant, Citrine (20), using x-ray crystallography and fluorescence spectroscopy in the pressure range 0.1–5 MPa. In this case ''function'' is understood to refer to fluorescence. Citrine was chosen for this study as its bright intrinsic fluorescence could be readily assayed under conditions similar to that required by crystallography. We previously reported a direct correlation between a progressive subangstrom deformation of the Citrine chromophore and a corresponding change in the fluorescence spectrum of the molecule (13). In this study, we extend this work to describe how global structural changes in the larger protein matrix couple to the local deformation of the chromophore. Additionally, we report the pressure-induced structural changes that are responsible for a change in the fluorescence intensity.

The YFP family is distinguished from the *Aequorea* green fluorescent protein (GFP) family by the mutation T203Y. This mutation stacks a phenol ring $\approx$3.4 Å above the phenol ring of the wild-type main chromophore. The main chromophore is formed by the autocatalytic fusion of residues 65–67 and is referred to as residue 66. The weak interaction of the main chromophore and the phenol ring of Tyr^{203} is responsible for shifting the fluorescence peak of Citrine from green to yellow (18).

The majority of the Citrine scaffold is a β-barrel structure, approximately cylindrical with a diameter of $\approx$25 Å and a height of $\approx$50 Å (Fig. 1). Tyr^{203} forms part of the wall of the Citrine β-barrel, and its side chain, a phenol ring,

Submitted February 19, 2009, and accepted for publication June 24, 2009.

Nozomi Ando and Chae Un Kim contributed equally to this work.

*Correspondence: smg26@cornell.edu

Buz Barstow's present address is Department of Systems Biology, Harvard Medical School, Boston, MA 02115.

Nozomi Ando's present address is Department of Chemistry, Massachusetts Institute of Technology, Cambridge, MA 02139.

Editor: Enrico Gratton.

0006-3495/09/09/1719/9 $2.00

doi: 10.1016/j.bpj.2009.06.039

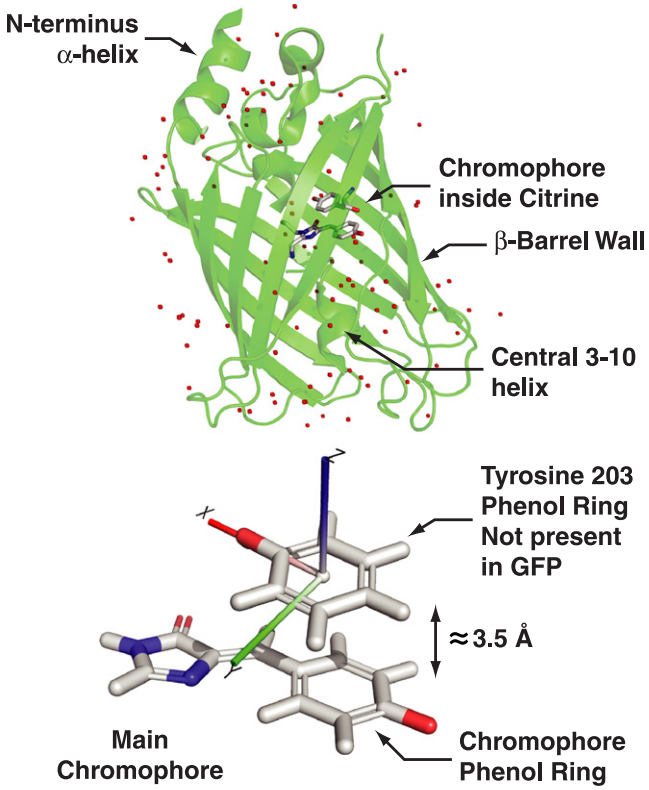

FIGURE 1 Ribbon diagram of the Citrine molecule and chromophore. The chromophore consists of the main chromophore and Tyr^{203}. The coordinate axes embedded in the Tyr^{203} phenol are used in the discussion in this article.

projects into the interior of the β-barrel. The main chromophore is attached to a 3-10 helix that threads through the center of the β-barrel. The top and bottom of the β-barrel consist of loops and the N-terminus α-helix.

We showed previously that the pressure-induced reorientation of the main chromophore and the Tyr^{203} phenol leads to a shift in the fluorescence peak of the Citrine from 527 nm at ambient pressure to 510 nm at pressures >350 MPa (13). As the pressure applied to Citrine is increased from ambient pressure to 500 MPa, the main chromophore moves continuously by $\approx$0.5 Å in the positive y-direction shown in Fig. 1 and $\approx$0.4 Å in the positive x-direction from its ambient pressure position relative to Tyr^{203}. This small deformation removes the perturbing influence of Tyr^{203} and permits the main chromophore to return to its green fluorescent state. An estimate of the effect of removing this perturbation on the fluorescence peak of Citrine is included in Section S1 of the Supporting Material.

To understand what global structural changes in the scaffold of Citrine are responsible for the local deformation observed at the chromophore, we analyzed the motion of individual residues as well as groups of residues in the crystal structures obtained at high pressure. The results of this analysis show that the chromophore motion is actuated by the concerted, differential motion of two groups of residues in the β-barrel wall and central 3-10 helix of the Citrine molecule. These results support the view that small global changes to the structure of a protein can be communicated to the active site and greatly affect its function. They also suggest that protein function may be modified by introducing mutations that affect the relative positions and motion of clusters of residues that may exist within a single domain of the protein.

EXPERIMENTAL PROCEDURES

Crystals of Citrine were grown as described previously (13). A closely spaced series of high-pressure structures of Citrine were solved using the high-pressure cryocooling x-ray crystallography technique developed by Kim et al. (8). Briefly, a protein crystal is pressurized with helium gas and is then cooled to 77 K, locking in collective pressure-induced structural changes (8,9). After pressure release, the protein molecules composing the crystal will retain many of the collective changes of the pressurized state, as long as the crystal temperature remains well below the protein glass transition temperature (9,14,21). Citrine crystals were prepared at pressures ranging from 50 to 500 MPa (13). Each structure at every pressure is derived from a different crystal at cryogenic temperatures. The high resolution limit of the datasets was typically <2 Å (13). The Citrine structures used in this analysis are listed in Table S1.

The fluorescence spectra of high-pressure cryocooled Citrine samples were recorded using a custom microspectrophotometer described previously (13). As the fluorescence spectra of YFPs are known to be sensitive to changes in solution pH (22), the choice of buffer was considered carefully. Citrine displayed a similar response to pressure under various buffers at room temperature (Section S2 of the Supporting Material), in agreement with reports that Citrine is less sensitive to changes in pH than other *Aequorea* YFPs (20). Nonetheless, buffers with low volume changes of ionization were selected to stabilize the pH for crystallization and spectroscopy (23,24).

To calculate the overall volume reduction of Citrine, the external surface and surfaces of internal cavities present in each solvent-stripped structure were identified and traced with the reduced surface computation program MSMS (25) using a 1.2 Å radius probe. The surfaces identified by MSMS were used to compute the volume enclosed by the external surface of each Citrine structure (the excluded volume) and the volumes of the cavities present in the interior of each Citrine structure. The net volume of each structure was computed by subtracting the total internal cavity volume from the excluded volume of the structure.

Clusters of residues that move in concert with increasing pressure in the series of Citrine atomic structures were identified using the heuristic clustering algorithm, RIGIMOL (DeLano Scientific LLC, Palo Alto, CA). Input coordinate files to RIGIMOL were prepared with PyMOL (DeLano Scientific LLC). Structural properties of Citrine atomic structures such as inertia tensors, centers of mass, and principal axes were computed using custom software implemented in PYTHON with use of the NUMPY numerical library. Fitting of structural parameters was carried out using the IPYTHON program and the NUMPY and SCIPY numerical libraries. Detailed discussion of the clustering algorithm and inertia tensor analysis can be found in Section S3 of the Supporting Material.

RESULTS

Nonisotropic volume reduction of Citrine under pressure

The deformation of Citrine due to pressure is very small in comparison to the overall dimension of the molecule. The

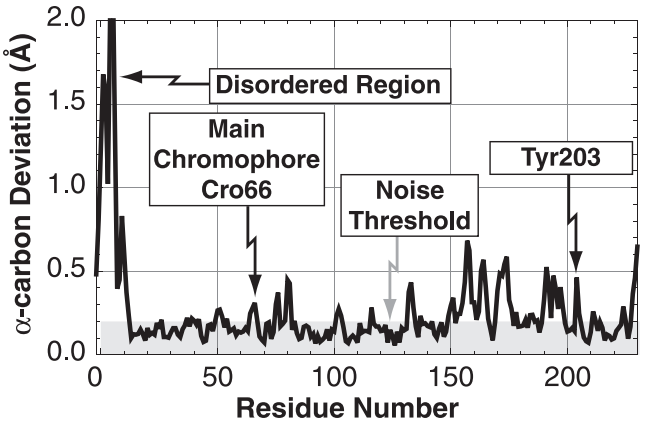

FIGURE 2 Average distance deviation between α-carbons of Citrine at 0.1 and 400 MPa versus residue number. Deviations below the gray band at 0.2 Å are at the uncertainty of the measurement.

superimposed structures of Citrine at 0.1 and 400 MPa are shown in Fig. S6. The overall volume of Citrine decreased by ~300 $Å^3$, or 1.1%, over the 500 MPa pressure range investigated (Section S4 and Fig. S7 of the Supporting Material), consistent with reported values of protein compressibility (26). The displacement of the α-carbons over this pressure range is small in magnitude when compared to the overall dimension of the protein. A plot of the average displacement of the α-carbon of each residue under a pressure increase from ambient pressure to 400 MPa is shown in Fig. 2. We estimate that the uncertainty in the displacements of the α-carbons is $\approx$0.2 Å, as indicated by the apparent ''noise threshold'' in Fig. 2 (9,11). In addition to the displacements seen at the disordered N-terminus of Citrine, there are numerous residues that were displaced by several times the noise threshold. Two notable displacements highlighted in Fig. 2 are the pressure-induced displacements of the main chromophore and Tyr^{203}, consistent with our previous report of the deformation of the chromophore (13). It is important to emphasize that although there are likely many residues in the structure of Citrine where the displacement due to pressurization is $<$0.2 Å, the positional uncertainties (27) on the Citrine structures do not permit the definitive identification of displacements smaller than the noise threshold (9,11) (Section S5 and Table S1 of the Supporting Material).

It is noted that the magnitudes of the residue displacements are nonuniform, suggesting the nonisotropic nature of the compression of Citrine, despite Citrine's overall linear volume reduction with pressure (Section S4 and Fig. S7 of the Supporting Material). Consistent with this, a distance difference matrix of the structures at 0.1 and 400 MPa show both the contraction and expansion of distances between residue pairs (Section S6 and Fig. S8 of the Supporting Material). If the compression of Citrine under high pressure were isotropic and homogeneous, we would expect that the relative orientation of the two elements of the chromophore would be retained with increasing pressure. However, the two chromophore elements slide apart with very little change in vertical separation with increasing pressure (13).

Principal axis and clustering analysis of Citrine compression

To further quantify the nonisotropic compression of Citrine, we analyzed the relative motion of clusters of atoms in the series of high-pressure Citrine structures. The β-barrel and the central 3-10 helix of Citrine were extracted from the series of high-pressure structures and aligned using the least squares fitting algorithm incorporated into PyMOL. The clustering algorithm RIGIMOL was used to identify clusters of atoms that move in concert with increased pressure. This analysis was restricted to the β-barrel and central 3-10 helix to avoid domination of the analysis by the disordered regions of the protein. The identification of clusters was found to be very reproducible, largely independent of choice of input structures (RIGIMOL can only take one structure per pressure as input), clustering algorithm parameters, and structural refinement method. (A description of the validation tests carried out on the RIGIMOL algorithm may be found in Section S3 of the Supporting Material.)

The clustering algorithm identified two clusters of atoms in the β-barrel and central 3-10 helix of Citrine that move with respect to one another as the pressure applied to the Citrine molecule is increased (Fig. 3). An important feature of the cluster assignment is that the perturbing Tyr^{203} is attached to cluster 1, whereas the main chromophore is attached to cluster 2. Over the investigated pressure range, the center of mass of cluster 1, containing the perturbing Tyr^{203} ring, moves by ≈ -0.2 Å in the x-direction with respect to that of cluster 2, which contains the main chromophore. For ease of reference, the coordinate axes used in this discussion are the same as those used by us in our prior work on the deformation of the chromophore of Citrine (13). This coordinate system is shown in Figs. 1 and 5. The cluster 1 center of mass appears to move relative to cluster 2 in the y-direction. However, this y-direction motion is small in comparison to the uncertainty on this motion, especially the displacement at 400 MPa. For this reason, it is difficult to discern if this motion is linear, perhaps extending to ≈ -0.05 Å by 500 MPa, or curved; returning to $\approx$0.0 Å at 500 MPa. There is no discernible motion in the z-direction.

Principal axis analysis shows that another component of the cluster movement is rotation. The principal axes of each cluster were found by computing the eigenvectors of the cluster's inertia tensor using the NUMPY numerical library. The principal axes were shown to rotate relative to one another by 1°–2° over 500 MPa (Figs. 4 and 5), suggesting a slight bending of the Citrine β-barrel wall. Consistent with this bending, principal axis analysis of the entire β-barrel wall suggests a redistribution of mass toward the side of the β-barrel wall containing Tyr^{203} (Section S7 of

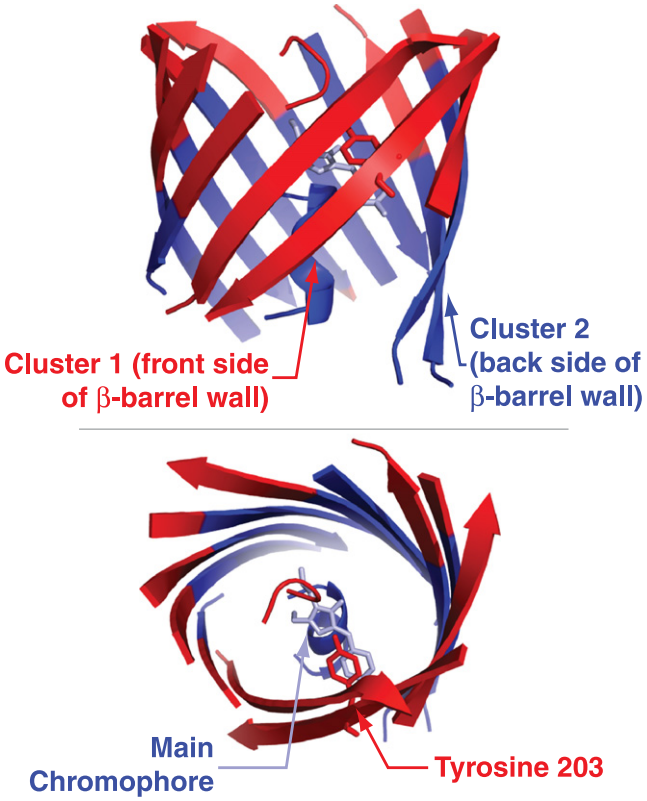

FIGURE 3 Clusters identified in the β-barrel walls and central 3-10 helix of the Citrine molecule that move in concert under high-pressure perturbation. Note that the main chromophore is attached to cluster 2, whereas the perturbing Tyr^{203} ring is attached to cluster 1. The main chromophore is colored light blue.

the Supporting Material). To investigate the effect of cluster motion on the chromophore, the pressure-induced translation and rotation of cluster 1 relative to cluster 2 were extracted and applied to Tyr^{203} of the ambient pressure structure, keeping the main chromophore fixed. Under these operations, Tyr^{203} moved in the negative x- and y-directions with respect to the main chromophore, consistent with the actual direction of movement observed at high pressure (13) (Fig. 5). This result suggests that the cluster translation, coupled with the slight rotation of the principal axes of the clusters, could possibly produce sufficient leverage to actuate the relative motion of the two elements of the Citrine chromophore.

Perturbation of hydrogen bonding network in chromophore cavity

We reported previously that the fluorescence peak of Citrine shifts to the blue with increasing pressure (13). Accompanying this blue-shift is a considerable reduction in fluorescence intensity, implying either a reduction in the quantum yield, a change in the absorption spectrum of Citrine, or both. The fluorescence peak intensity of Citrine solutions, high-pressure cryocooled at a range of pressures from 50 to 360 MPa, is shown in Fig. 6. The fluorescence peak intensity initially increases, from 0.1 MPa to 50 MPa, and then decreases. By a pressure of 200 MPa, the peak Citrine fluorescence intensity is $\approx$1/100th of its value at 50 MPa. Reports by Mauring et al. (28) and Ganesan et al. (29) suggest that the fluorescence intensity of Citrine may be modulated by the length of the hydrogen bond between the chromophore phenolic oxygen and the δ_1-nitrogen of His^{148}. The His^{148} δ_1-nitrogen to chromophore phenolic oxygen bond increases by 0.4 Å under a pressure increase from 0.1 to 500 MPa (Fig. 7).

In addition to the His^{148} δ_1-nitrogen to chromophore phenolic oxygen bond, the main chromophore is stabilized by several other hydrogen bonds. A simplified schematic of the hydrogen-bonding network stabilizing the Citrine

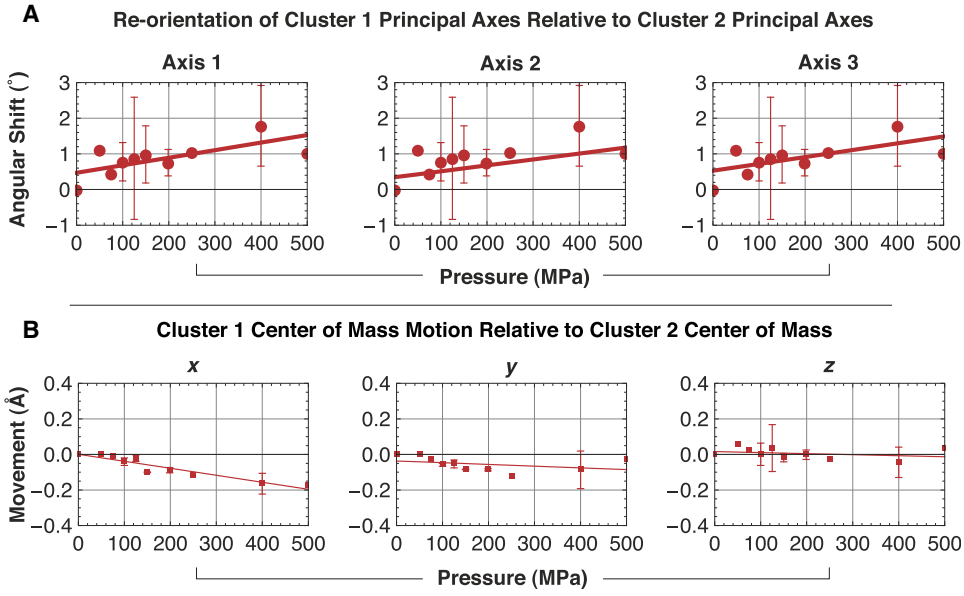

FIGURE 4 (*A*) Rotation of the principal axes of cluster 1 in a reference frame where the principal axes of cluster 2 are fixed. The angular shift is the angle formed between the principal axis at a given pressure and the principal axis at 0.1 MPa. (*B*) Motion of the center of mass of cluster 1 from its ambient pressure position in a reference frame where the cluster 2 center of mass is fixed. The directions of the coordinate axes of this system are shown in Figs. 1 and 5. Linear fit lines in all plots were determined by least squares fitting with the NUMPY numerical library. The fit lines are intended to help guide the eye and do not imply linear behavior.

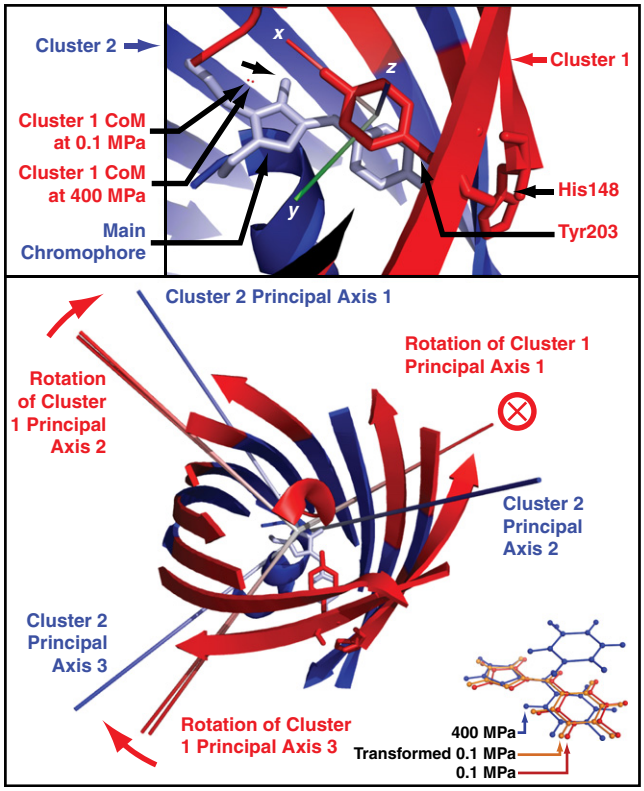

FIGURE 5 (*Upper panel*) Motion of the cluster 1 (*red*) center of mass in a reference frame where the center of mass of cluster 2 (*blue*) is fixed. (*Lower panel*) Rotation of cluster 1 principal axes relative to cluster 2 axes. The circled cross (⊗) next to cluster 1 principal axis 1 indicates that the rotation of the axis is into the figure. The main chromophore is colored in light blue for emphasis.

chromophore is shown in Fig. S10 *A*. Plots of behavior of other bonds in the chromophore cavity are shown in Fig. S10 *B*. A description of the behavior of the other bonds under pressure may be found in Section S8 of the Supporting Material.

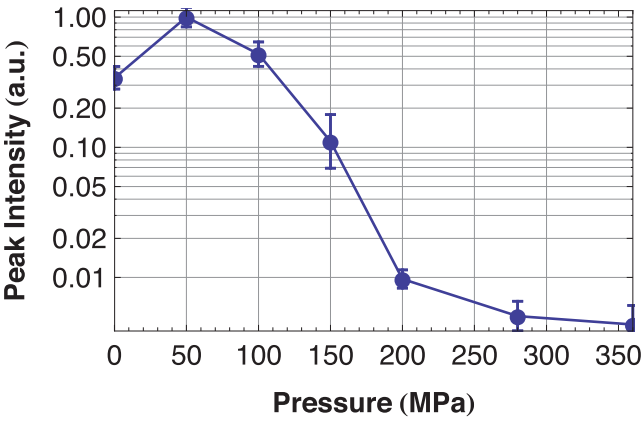

FIGURE 6 Fluorescence peak intensity of high-pressure cryo-cooled Citrine solution samples.

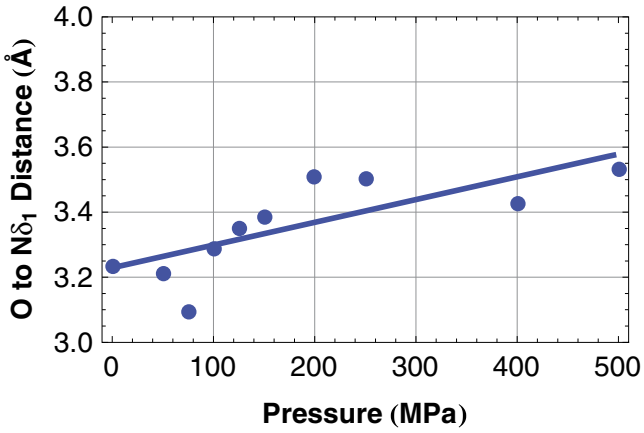

FIGURE 7 His^{148} δ_1-nitrogen to chromophore phenolic oxygen hydrogen bond length.

DISCUSSION

Reduction in fluorescence intensity with increasing pressure

Experiments on other *Aequorea* fluorescent protein (AFP) mutants suggest that the reduction in fluorescence intensity of Citrine under high-pressure cryocooling (Fig. 6) may be due to pressure-induced disruption of the chromophore cavity hydrogen-bonding network (18). This network serves to anchor the main chromophore, stabilizing the chromophore excited state, preventing nonradiative decay and facilitating the high quantum yield of the molecule (28). Niwa et al. (30) noted that certain analogs of the GFP chromophore (isolated from the β-barrel) absorb light yet are nonfluorescent at room temperature, but when frozen to cryogenic temperatures become fluorescent (30). Computer simulations indicate that in vacuum, the chromophore is fluorescent, whereas in liquid, the excited state of the molecule de-excites by quenching (31). Mauring et al. (28) showed that the application of high pressure to an *Aequorea* blue fluorescent protein (BFP) increased the quantum yield of the molecule. The central residue of the BFP chromophore is a histidine, a shorter residue than the tyrosine normally found at the center of an AFP chromophore. This shortened chromophore is unable to link to the chromophore cavity hydrogen-bonding network, leading to destabilization of the chromophore excited state. As a result, BFPs display lower quantum yields than other AFPs (28). Mauring et al. (28) attributed the pressure-induced increase in the quantum yield to the reattachment of the BFP chromophore to the chromophore cavity hydrogen-bonding network as the cavity was compressed.

Although the behavior of Citrine and EYFP (enhanced YFP) (32) under high pressure is the opposite of BFP (the fluorescence intensity reduces), the structural mechanism may be the same (perturbation of the chromophore cavity hydrogen-bonding network). The mutation H148V in YFP

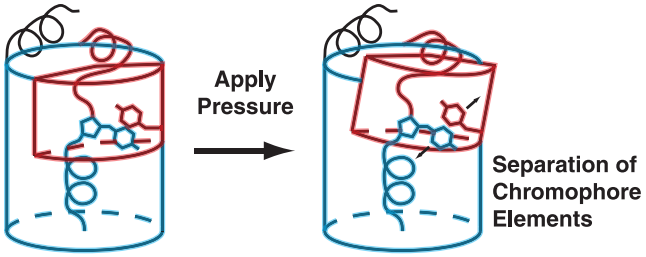

FIGURE 8 Cartoon representation of the bending of the Citrine scaffold.

removes a critical link in the hydrogen-bonding network attaching the phenolic oxygen of the main chromophore to the His^{148} δ_1-nitrogen and results in an 82% reduction in the fluorescence intensity with only a 15% drop in absorption (29). We speculate that the pressure-induced increase in this bond length is responsible for the reduction in fluorescence intensity of Citrine shown in Fig. 6.

Shifts in the absorption and fluorescence peaks of Citrine with increasing pressure at room temperature (Fig. S1) indicate that the Citrine absorption and fluorescence peaks maintain a constant Stokes shift. If this behavior is maintained at low temperature, then the absorption peak should blue-shift with increasing freezing pressure. As the high-pressure cryocooled Citrine solutions studied here were excited at 473 nm, the blue edge of Citrine absorption spectrum (the absorption peak at 0.1 MPa is 514 nm), we would expect absorption to increase with increasing freezing pressure. Thus, we speculate that the reduction in quantum yield of Citrine may be even greater than is implied by the reduction in fluorescence intensity seen in Fig. 6.

Deformation of the Citrine scaffold

The deformation of the Citrine scaffold can be thought of as the slight bending of the β-barrel scaffold. A cartoon representation of this deformation is shown in Fig. 8. As the pressure applied to the molecule is increased, the main chromophore remains anchored to cluster 2, attached to the central helix. However, the side of the β-barrel wall containing the perturbing Tyr^{203} ring and stabilizing His^{148} residue, moves away from cluster 2, carrying these two important residues with it. The large expansion of the distance from the central 3-10 helix to the wall of β-barrel in the vicinity of Tyr^{203} can be seen in the highlighted region in the distance difference matrix in Fig. S8.

It is interesting to note that the fluorescence peak intensity of all AFPs studied under pressure (13,32) increases with applied pressure, with the exception of the YFP types. The unusual pressure response of the YFPs at room temperature (32) and at cryogenic temperatures (13), may plausibly be due to a YFP structure that predisposes the YFP-type molecules to the bending behavior observed here.

There is no evidence that the crystalline environment significantly affects the fluorescence properties of the Citrine molecule relative to a solution of Citrine at equivalent concentration. The high optical density and overlapping absorption and fluorescence spectra of Citrine crystals, all of which had slightly different sizes, made it difficult to reproducibly measure the position of the peak of the fluorescence spectra of pressure cooled Citrine crystals. Thus, we were forced to seek a substitute: pressure cooled solutions in capillaries (13). The fluorescence spectra of a very small, flash frozen Citrine crystal and a flash frozen dilute solution of Citrine are plotted in Fig. S11 for comparison. The similarity of these two spectra suggests that the crystalline environment does not significantly perturb the fluorescence properties of Citrine. As pressure-induced unfolding is not expected to occur in the solution state of Citrine below at least 1000 MPa (33), it is plausible that the pressure effects captured in the crystalline state represents those in the solution state within the explored pressure range. This is reasonable as the deformation of Citrine in the crystal state is not a response to a directionally applied external force. As opposed to typical small molecule crystals, the fluid water channels intrinsic to most protein crystals constitute approximately half of the crystal mass and transmit hydrostatic pressure to each protein. A force originating at the surface of the crystal is not transmitted through covalent or metal bonds from molecule to molecule as happens in a small molecule crystal or a metal. There is no pressure gradient across the volume of the crystal: identical, uniform hydrostatic pressure is transmitted by the solvent channels to each molecule. Thus, the protein deformation in response to pressure is not due to an externally applied force per se; rather it results from pressure-dependent interactions of the molecule.

For example, it is known that the degree of ionization (34), hydration (34,35), and hydrogen bonding (34,36) of many amino acid residues are pressure dependent. It has also been shown that pressure changes the water occupancy of internal cavities (10,11,37,38). One expects that as these interactions change with pressure, the conformation of the protein will change in response. The fact that pressure is transmitted to the individual molecules in the crystal also argues that the resulting deformations are similar to those expected for the same molecule in solution, and differ only in so far as molecular contacts in the crystal change the surface exposure to water or constrain large deviations in protein structure. This belief is supported by earlier observation that both crystals and solutions of Citrine display the same release in the blue-shifting effects of pressure when warmed above the glass transition temperature and then recooled (13). This suggests that the structures of Citrine in the crystal and in solution do not diverge at elevated pressure. This contention is further supported by the similar response to pressure of the structure of hen egg-white lysozyme when measured by x-ray crystallography (6) and by high-pressure solution NMR (4).

At room temperature, the main chromophore of YFP protrudes slightly further, by $\approx$0.9 Å, into the chromophore

cavity than the chromophore in the EGFP structure (18). This preexisting deformation, possibly induced by the presence of the perturbing Tyr^{203} residue, may slightly weaken the YFP structure and predispose it to the bending behavior seen under high-pressure cryocooling. This bending behavior may be analogous to macroscopic structures failing at the weakest point.

Although the structure of Citrine and the response of its structure to high pressure are no doubt subtly different to that of wild-type GFP (wtGFP), the extension in path length from the phenolic oxygen to the ε_2-oxygen of Glu^{222} (Fig. S10) may also provide a framework for explaining the subtle pressure-induced red-shift in fluorescence peak of wtGFP (39). In the Citrine structures presented here, the distance from the phenolic oxygen of the main chromophore to the HOH-1 solvent molecule to the ε_2-oxygen of Glu^{222} increases by $\approx$0.5 Å from ambient pressure to 500 MPa. The increase in this distance should have no impact on the fluorescence properties of Citrine as excited state proton transfer from the main chromophore to Glu^{222} seems to play no role in the fluorescence mechanism of AFPs mutants containing phenolate anion chromophores (19). However, excited state proton transfer does play a role in the fluorescence mechanism of wtGFP, and the extension of the proton transfer path may be responsible for modification of the fluorescence properties of wtGFP under pressure (40,41).

An important observation from our earlier work (13) is that the fluorescence peak of Citrine approaches 510 nm, the fluorescence peak of EGFP under ambient conditions, as the pressure applied to the molecule is raised to >350 MPa. This shift to the green of the fluorescence peak is due to the removal of the perturbing effect of Tyr^{203} from the main chromophore (13). The results presented in this study, on the effect of high pressure on the scaffold of Citrine, indicate that the relative sliding motion of the Tyr^{203} phenol ring and the main chromophore is actuated by the separation of two clusters that compose the β-barrel wall and central 3-10 helix. This observation may provide a structural explanation for the observation of Blum et al. (42) that a single molecule of YFP (19,20) occasionally becomes dark, and then adopts a spectrum closely resembling the spectrum of bulk EGFP (19,43,44), before returning to a spectrum close to that of bulk YFP. It is known that many protein molecules fluctuate between a number of conformations (45). We speculate that at room temperature, YFPs may occasionally adopt a configuration structurally similar to the bent state seen at high-pressure. The bent scaffold of this state may transiently stabilize the main chromophore-Tyr^{203} separation needed for the molecule to fluoresce in the green. Single molecule experiments indicate that single enzymes display a range of catalytic rates (46,47), and switch between them, in much the same way that a single YFP molecule switches between several spectra (42). This result suggests that the high-pressure cryocooling technique may be useful for accessing the atomic structures of transiently populated enzyme states that are presently only observable in single molecule experiments. Experiments by Urayama et al. (9) indicated that high pressure stabilizes the structure of a room temperature conformational and functional substate of myoglobin. It is possible that the dark state of YFP observed by Blum et al. (42) is one in which the stabilizing interaction between the main chromophore and His^{148} is completely lost.

The structural information available on Citrine at high pressure may inspire structural modifications to Citrine that may permit the Citrine molecule to remain in the blue-shifted transient state for longer, or even permanently stabilize it. It may be possible to induce the bending of the Citrine scaffold seen at high-pressure under ambient conditions by repacking the Citrine scaffold by mutating or adding residues along the interface of these two clusters. On this basis, Fig. S12 shows several possible sites where one would logically seek to introduce mutations. To replicate the bending seen at high pressure, it is required that cluster 1 move down and to the right in the Fig. S12. It is interesting to consider if this may be achieved by simultaneously mutating residues on the left hand interface between clusters 1 and 2 to bulkier residues, and mutating those on the right hand interface to less bulky residues, while keeping other properties of the residues as similar as possible. On the left hand side, possible mutations may be Phe^{46} to Tyr or Trp, Val^{16} to Leu, Ile, or Met, Asn^{121} to Gln, Val^{112} to Leu, Ile, or Met, Tyr^{92} to Trp. On the right hand side, these mutations may be Ile^{161} to Val, Ala, or Gly, Gln^{183} to Asp, Cys, Thr, or Ser, Val^{163} to Ala or Gly, leaving Phe^{165} unchanged as it is the smallest aromatic amino acid. The success of this strategy would depend on the perturbations of these mutations being small enough to not affect the folding of the β-barrel scaffold. Although a blue-shifted YFP is of little practical value, it would be an important proof of principle. The same strategy may be applied to engineer new AFPs that can switch color in response to a trigger. Such a protein may be useful for single-molecule and imaging techniques. More significantly, if structural perturbations due to pressure of the character observed in Citrine are seen in catalytic proteins, it may be possible to introduce mutations similar to the ones suggested for Citrine to bias a population of catalytic molecules into more active conformations, resulting in an increase in the bulk rate of catalysis. Further discussion of this issue is included in Section S9.

CONCLUSIONS

We have shown that the scaffold of the Citrine molecule deforms under high-pressure. Rather than isotropically compressing, the high-pressure deformation of Citrine is nonhomogeneous. The Citrine β-barrel is approximately divided into two atomic clusters that move and rotate relative to one another under pressurization. The two elements of the Citrine chromophore, the perturbing Tyr^{203} ring and the main chromophore, are each attached to different clusters.

The relative motion and rotation of these two clusters causes a deformation in the Citrine scaffold that is reminiscent of bending, actuating the separation of the two elements of the Citrine chromophore, resulting in a fluorescence shift of the molecule. In addition to actuating the fluorescence shift of the molecule, the bending of the Citrine scaffold also perturbs the hydrogen-bonding network stabilizing the main chromophore. The most important consequence of this perturbation is an increase in the distance from the main chromophore phenol to the His^{148} side chain. The increase in the His^{148} to main chromophore distance may plausibly result in a destabilization of the excited state of the chromophore and the consequent dimming of Citrine seen under high-pressure cryocooling conditions (13) and under high hydrostatic pressure (32).

The bent state of the Citrine scaffold may be highly structurally similar to the transiently observed blue-shifted state of YFP at ambient pressure (42). This suggests that high-pressure x-ray crystallography may offer the possibility of solving the structures of transiently occupied enzymatic states and understanding the structural basis of their differing catalytic rates. These high-pressure structures of Citrine may inspire mutations that permit Citrine to remain in the blue-shifted state for longer periods of time.

Finally, these experiments explicitly demonstrate the continuous linkage of a protein scaffold and activity (fluorescence in this case) of the protein. Studies of the effects of pressure on the structure and function of protein molecules yield several insights into the structure-function relationship of these molecules. First, these studies probe the energy landscapes of protein active sites and offer what we believe is new insight on the structural basis of enzymatic catalysis. Second, these studies illustrate the coupling of protein active sites and the protein matrix, giving additional insights into the structural basis of allosteric behavior, especially in monomeric proteins. Third, these experiments may provide structural explanation of the results of single molecule experiments, by allowing the trapping of normally transiently occupied protein states, as we believe was shown with Citrine. Fourth, these studies may highlight the tunability of protein, especially enzymatic activity, and suggest avenues for improving the function of protein molecules under ambient conditions that may not be highlighted by single protein structures, random mutagenesis, or directed evolution methods.

SUPPORTING MATERIAL

Nine sections, a table, and 12 figures are available at http://www.biophysj.org/biophysj/supplemental/S0006-3495(09)01215-6.

The authors thank Dr. Cynthia Kinsland and the staff of the Cornell Life Sciences Core Lab Centers Protein Facility for assistance with the modification and expression of Citrine vectors, and protein purification and the MacCHESS staff at the Cornell High Energy Synchrotron Source (CHESS) for assistance in data collection and reduction (MacCHESS is the macromolecular division of CHESS). We thank Martin Novak for invaluable assistance with the construction of experiments, Yi-Fan Chen and Dr. Mark Tate (Cornell University) for the construction of the internals of the high pressure cryocooling apparatus, Odin Wojcik and AccuFab Inc. (Ithaca, NY) for the construction of the high pressure cryocooling safety enclosure, Professor Warren Zipfel (Cornell University) for providing a sample of monomeric EGFP, Professor Roger Tsien (University of California, San Diego) for providing the Citrine plasmid, Dr. Gerhard Hummer (National Institute of Diabetes and Digestive and Kidney Diseases), Dr. Ismail Hafez (University of British Columbia, Vancouver), Professors Lois Pollack and Brian Crane (Cornell University) for useful discussions, Professor Robert Campbell (University of Alberta) for assistance with crystallization of Citrine, Elizabeth Landrum and Darren Southworth for assistance in data collection and Joan Lenz and Dr. Raymond Molloy (Cornell University) for assistance with molecular biology.

This work is supported by the Department of Energy/ Biological and Environmental Research (FG02-97ER62443), and National Institutes of Health Protein Structure Initiative (GM074899). CHESS is supported by the National Science Foundation and National Institutes of Health via National Science Foundation award DMR-0225180, and MacCHESS is supported via National Institutes of Health grant RR001646.

REFERENCES

1. Perutz, M. F., G. Fermi, B. Luisi, B. Shaanan, and R. C. Liddington. 1987. Stereochemistry of cooperative mechanisms in hemoglobin. *Acc. Chem. Res.* 20:309–321.
2. Schirmer, T., and P. R. Evans. 1990. Structural basis of the allosteric behavior of phosphofructokinase. *Nature*. 343:140–145.
3. Long, S. B., X. Tao, E. B. Campbell, and R. Mackinnon. 2007. Atomic structure of a voltage-dependent K^+ channel in a lipid membrane-like environment. *Nature*. 450:376–382.
4. Refaee, M., T. Tezuka, K. Akasaka, and M. P. Williamson. 2003. Pressure-dependent changes in the solution structure of hen egg-white lysozyme. *J. Mol. Biol.* 327:857–865.
5. Fourme, R., E. Girard, R. Kahn, I. Ascone, M. Mezouar, et al. 2003. Using a quasi-parallel x-ray beam of ultrashort wavelength for high-pressure virus crystallography: implications for standard macromolecular crystallography. *Acta Crystallogr. D Biol. Crystallogr.* 59:1767–1772.
6. Kundrot, C., and F. Richards. 1987. Crystal structure of hen egg-white lysozyme at a hydrostatic pressure of 1000 atmospheres. *J. Mol. Biol.* 193:157–170.
7. Kundrot, C., and F. Richards. 1986. Collection and processing of x–ray diffraction data from protein crystals at high pressure. *J. Appl. Cryst.* 19:208–213.
8. Kim, C. U., R. Kapfer, and S. M. Gruner. 2005. High-pressure cooling of protein crystals without cryoprotectants. *Acta Crystallogr. D Biol. Crystallogr.* 61:881–890.
9. Urayama, P. K., G. N. Phillips, and S. M. Gruner. 2002. Probing substates in sperm whale myoglobin using high-pressure crystallography. *Structure*. 10:51–60.
10. Collins, M. D., G. Hummer, M. L. Quillin, B. W. Matthews, and S. M. Gruner. 2005. Cooperative water filling of a nonpolar protein cavity observed by high-pressure crystallography and simulation. *Proc. Natl. Acad. Sci. USA*. 102:16668–16671.
11. Collins, M. D., M. L. Quillin, G. Hummer, B. W. Matthews, and S. M. Gruner. 2007. Structural rigidity of a large cavity-containing protein revealed by high-pressure crystallography. *J. Mol. Biol.* 367:752–763.
12. Williamson, M. P., K. Akasaka, and M. Refaee. 2003. The solution structure of bovine pancreatic trypsin inhibitor at high pressure. *Protein Sci.* 12:1971–1979.
13. Barstow, B., N. Ando, C. U. Kim, and S. M. Gruner. 2008. Alteration of citrine structure by hydrostatic pressure explains the accompanying spectral shift. *Proc. Natl. Acad. Sci. USA*. 105:13362–13366.
14. Frauenfelder, H., N. A. Alberding, A. Ansari, D. Braunstein, B. R. Cowen, et al. 1990. Proteins and pressure. *J. Phys. Chem.* 94:1024–1037.

15. Ueda, I., H. Minami, H. Matsuki, and T. Inoue. 1999. Does pressure antagonize anesthesia? High-pressure stopped-flow study of firefly luciferase and anatomy of initial flash. *Biophys. J.* 76:478–482.

16. Unno, M., K. Ishimori, and I. Morishima. 1990. High-pressure laser photolysis study of hemoproteins. Effects of pressure on carbon monoxide binding dynamics for R- and T-state hemoglobins. *Biochemistry.* 29:10199–10205.

17. Hay, S., M. J. Sutcliffe, and N. S. Scrutton. 2007. Promoting motions in enzyme catalysis probed by pressure studies of kinetic isotope effects. *Proc. Natl. Acad. Sci. USA.* 104:507–512.

18. Wachter, R. M., M. Elsliger, K. Kallio, G. T. Hanson, and S. J. Remington. 1998. Structural basis of spectral shifts in the yellow-emission variants of green fluorescent protein. *Structure.* 6:1267–1277.

19. Tsien, R. Y. 1998. The green fluorescent protein. *Annu. Rev. Biochem.* 67:509–544.

20. Griesbeck, O., G. S. Baird, R. E. Campbell, D. A. Zacharias, and R. Y. Tsien. 2001. Reducing the environmental sensitivity of yellow fluorescent protein. Mechanism and applications. *J. Biol. Chem.* 276:29188–29194.

21. Kim, C. U., Y. Chen, M. W. Tate, and S. M. Gruner. 2007. Pressure induced high-density amorphous ice in protein crystals. *J. Appl. Cryst.* 41:1–7.

22. Elsliger, M. A., R. M. Wachter, G. T. Hanson, K. Kallio, and S. J. Remington. 1999. Structural and spectral response of green fluorescent protein variants to changes in pH. *Biochemistry.* 38:5296–5301.

23. Neuman, R., W. Kauzmann, and A. Zipp. 1973. Pressure dependence of weak acid ionization in aqueous buffers. *J. Phys. Chem.* 77:2687–2691.

24. Zipp, A., and W. Kauzmann. 1973. Pressure denaturation of metmyoglobin. *Biochemistry.* 12:4217–4228.

25. Sanner, M. F., A. J. Olson, and J. C. Spehner. 1996. Reduced surface: an efficient way to compute molecular surfaces. *Biopolymers.* 38:305–320.

26. Heremans, K., and L. Smeller. 1998. Protein structure and dynamics at high pressure. *Biochim. Biophys. Acta.* 1386:353–370.

27. Cruickshank, D. 1999. Remarks about protein structure precision. *Acta Crystallogr. D Biol. Crystallogr.* 55:583–601.

28. Mauring, K., J. Deich, F. I. Rosell, T. B. McAnaney, W. E. Moerner, et al. 2005. Enhancement of the fluorescence of the blue fluorescent proteins by high pressure or low temperature. *J. Phys. Chem. B.* 109:12976–12981.

29. Ganesan, S., S. M. Ameer-Beg, T. T. Ng, B. Vojnovic, and F. S. Wouters. 2006. A dark yellow fluorescent protein (YFP)-based resonance energy-accepting chromoprotein (REACh) for Forster resonance energy transfer with GFP. *Proc. Natl. Acad. Sci. USA.* 103:4089–4094.

30. Niwa, H., S. Inouye, T. Hirano, T. Matsuno, S. Kojima, et al. 1996. Chemical nature of the light emitter of the Aequorea green fluorescent protein. *Proc. Natl. Acad. Sci. USA.* 93:13617–13622.

31. Toniolo, A., S. Olsen, L. Manohar, and T. Martínez. 2004. Conical intersection dynamics in solution: the chromophore of green fluorescent protein. *Faraday Discuss.* 127:149–163.

32. Verkhusha, V. V., A. E. Pozhitkov, S. A. Smirnov, J. W. Borst, A. van Hoek, et al. 2003. Effect of high pressure and reversed micelles on the fluorescent proteins. *Biochim. Biophys. Acta.* 1622:192–195.

33. Scheyhing, C. H., F. Meersman, M. A. Ehrmann, K. Heremans, and R. F. Vogel. 2002. Temperature-pressure stability of green fluorescent protein: a Fourier transform infrared spectroscopy study. *Biopolymers.* 65:244–253.

34. Mozhaev, V., K. Heremans, J. Frank, P. Masson, and C. Balny. 1996. High pressure effects on protein structure and function. *Proteins.* 24:81–91.

35. Gross, M., and R. Jaenicke. 1994. Proteins under pressure. The influence of high hydrostatic pressure on structure, function and assembly of proteins and protein complexes. *Eur. J. Biochem.* 221:617–630.

36. Le Tilly, V., O. Sire, B. Alpert, and P. T. Wong. 1992. An infrared study of 2H-bond variation in myoglobin revealed by high pressure. *Eur. J. Biochem.* 205:1061–1065.

37. Ando, N., B. Barstow, W. A. Baase, A. Fields, B. W. Matthews, et al. 2008. Structural and thermodynamic characterization of T4 lysozyme mutants and the contribution of internal cavities to pressure denaturation. *Biochemistry.* 47:11097–11109.

38. Hummer, G., S. Garde, A. E. García, M. E. Paulaitis, and L. R. Pratt. 1998. The pressure dependence of hydrophobic interactions is consistent with the observed pressure denaturation of proteins. *Proc. Natl. Acad. Sci. USA.* 95:1552–1555.

39. Oger, P. M., I. Daniel, and A. Picard. 2006. Development of a low-pressure diamond anvil cell and analytical tools to monitor microbial activities in situ under controlled P and T. *Biochim. Biophys. Acta.* 1764:434–442.

40. Leiderman, P., R. Gepshtein, I. Tsimberov, and D. Huppert. 2008. Effect of temperature on excited-state proton tunneling in wt-green fluorescent protein. *J. Phys. Chem. B.* 112:1232–1239.

41. Lill, M. A., and V. Helms. 2002. Proton shuttle in green fluorescent protein studied by dynamic simulations. *Proc. Natl. Acad. Sci. USA.* 99:2778–2781.

42. Blum, C., A. J. Meixner, and V. Subramaniam. 2004. Room temperature spectrally resolved single-molecule spectroscopy reveals new spectral forms and photophysical versatility of *Aequorea* green fluorescent protein variants. *Biophys. J.* 87:4172–4179.

43. Cubitt, A. B., R. Heim, S. R. Adams, A. E. Boyd, L. A. Gross, et al. 1995. Understanding, improving and using green fluorescent proteins. *Trends Biochem. Sci.* 20:448–455.

44. Brejc, K., T. K. Sixma, P. A. Kitts, S. R. Kain, R. Y. Tsien, et al. 1997. Structural basis for dual excitation and photoisomerization of the Aequorea victoria green fluorescent protein. *Proc. Natl. Acad. Sci. USA.* 94:2306–2311.

45. English, B., W. Min, A. Van Oijen, K. Lee, G. Luo, et al. 2006. Ever-fluctuating single enzyme molecules: Michaelis-Menten equation revisited. *Nat. Chem. Biol.* 2:87–94.

46. Min, W., B. P. English, G. Luo, B. J. Cherayil, S. C. Kou, et al. 2005. Fluctuating enzymes: lessons from single-molecule studies. *Acc. Chem. Res.* 38:923–931.

47. Kou, S., B. Cherayil, W. Min, B. English, and X. Xie. 2005. Single-molecule Michaelis-Menten equations. *J. Phys. Chem. B.* 109:19068–19081.